Flow (2021), 1–3
doi:10.1017/flo.2021.5

RESEARCH ARTICLE

Supplementary Material: Emergence of in-line swimming patterns in zebrafish pairs

Maurizio Porfiri[1,2,3*], Mert Karakaya[1], Raghu Ram Sattanapalle[1] and Sean D. Peterson[4]

[1]Mechanical and Aerospace Engineering Department, New York University Tandon School of Engineering, 6 MetroTech Center, Brooklyn, NY, 11201, USA
[2]Biomedical Engineering Department, New York University Tandon School of Engineering, 6 MetroTech Center, Brooklyn, NY, 11201, USA
[3]Center for Urban Science and Progress, New York University Tandon School of Engineering, 370 Jay Street, Brooklyn, NY, 11201, USA
[4]Mechanical and Mechatronics Engineering, University of Waterloo, 200 University Ave W, Waterloo, Ontario, N2L 3G1, Canada
*Corresponding author. E-mail: mporfiri@nyu.edu

Received: 8 November 2020; **Revised:** 23 March 2021; **Accepted:** 25 May 2021

1. Stability Analysis for A-dipoles

In addition to the case of a T-dipole examined in the main text, we consider an A-dipole, as per the definition of Kanso and Tsang (2014). The only difference between the two cases is in the form of the hydrodynamic turning, which now reads as

$$\Omega_f(t) = \hat{\boldsymbol{v}}_f^{\perp}(t) \cdot \left[\nabla \boldsymbol{U}_f(\boldsymbol{r}_f(t))\hat{\boldsymbol{v}}_f(t)\right], \tag{1}$$

which can be expanded as follows:

$$\Omega_f(t) = \pm\frac{2r_{0,\check{f}}^2 v_{0,\check{f}}}{\rho(t)^6}((-3\Delta x(t)^2\Delta y(t) + \Delta y(t)^3)\cos(2\theta_f(t) + \theta_{\check{f}}(t)) + (\Delta x(t)^3 - 3\Delta x(t)\Delta y(t)^2)\sin(2\theta_f(t) + \theta_{\check{f}}(t))), \tag{2}$$

where the plus (minus) sign is for f equal to 1 (2).

Using this expression for the hydrodynamic turning changes the stability analysis for in-line swimming, whose state matrix, upon following the exact steps of the main text, becomes

$$A_{\text{in-line}} = \left[\begin{array}{cccc|cccc} 0 & 0 & -\frac{2r_0^2 v_0}{d^3} & 0 & 0 & 0 & 0 & 0 \\ 0 & 0 & 0 & \frac{v_0}{d}\left(1+\frac{r_0^2}{d^2}\right) & v_0\left(1-\frac{r_0^2}{d^2}\right) & 0 & 0 & 0 \\ 0 & 0 & 0 & 0 & 0 & 0 & 0 & 0 \\ 0 & 0 & 0 & 0 & 0 & 0 & v_0\left(1+\frac{r_0^2}{d^2}\right) & 0 \\ \hline 0 & 0 & 0 & 0 & 0 & 1 & 0 & 0 \\ 0 & 0 & 0 & 0 & -k_p\eta d & -\eta & -\frac{\eta v_0}{d} + \frac{k_p\eta d}{2} + k_v\eta v_0 & -\frac{v_0}{d}\left(1+\frac{r_0^2}{d^2}\right) \\ 0 & 0 & 0 & 0 & 0 & 0 & 0 & 1 \\ 0 & 0 & 0 & 0 & \frac{12\eta v_0 r_0^2}{d^3} + 2k_p\eta d & 0 & -k_p\eta d - 2k_v\eta v_0 & -\eta \end{array}\right]. \tag{3}$$

In-line swimming is asymptotically stable if and only $A_{\text{in-line},22}$ is Hurwitz. Similar to the main text, by applying the Routh-Hurwitz criterion, we can learn about several interesting limit cases. Specifically, we find that: i) for d sufficiently large, in-line swimming is asymptotically stable; ii) for small values of d, in-line swimming is asymptotically unstable; iii) for η sufficiently large, large values of k_v will hinder stability, while the effect of k_p is modulated by d ($d < \sqrt{3}r_0$, large gains are detrimental to stability, while for $d > \sqrt{3}r_0$, they could guarantee stability).

The study of side-by-side swimming follows closely the previous analysis. However, there are some key differences between these schooling patterns. Unlike in-line swimming, side-by-side swimming requires a specific distance between the animals, which is obtained by balancing the repulsion from hydrodynamics with attraction due to social interactions, leading to $d = \sqrt[4]{\frac{2r_0^2 v_0}{k_p}}$. While maintaining this distance, the advective velocity is $\boldsymbol{U}_f(\boldsymbol{r}_f(t)) = -\frac{r_0^2 v_0}{d^2}\hat{\boldsymbol{i}}$ for $f \in \{1,2\}$, thereby slowing down the motion of the fish that will swim at a reduced speed of $v_0\left(1-\frac{r_0^2}{d^2}\right)$.

Similar to in-line swimming, we can derive the equations of motion for a perturbation about this nominal solution, that is,

$$A_{\text{side-by-side}} = \left[\begin{array}{cccc|cc|cc} 0 & 0 & 0 & 0 & 0 & \frac{2r_0^2 v_0}{d^3} & 0 & 0 \\ 0 & 0 & v_0\left(1+\frac{r_0^2}{d^2}\right) & 0 & \frac{2r_0^2 v_0}{d^3} & 0 & 0 & 0 \\ 0 & 0 & 0 & 1 & 0 & 0 & 0 & 0 \\ 0 & 0 & k_p\eta d & -\eta & k_p\eta & 0 & 0 & 0 \\ \hline 0 & 0 & 0 & 0 & 0 & 0 & 0 & 0 \\ 0 & 0 & 0 & 0 & 0 & 0 & v_0\left(1-\frac{r_0^2}{d^2}\right) & 0 \\ 0 & 0 & 0 & 0 & 0 & 0 & 0 & 1 \\ 0 & 0 & 0 & 0 & 0 & -\left(2k_p\eta+\frac{12\eta r_0^2 v_0}{d^4}\right) & k_p\eta d - 2k_v\eta v_0\eta & -\eta \end{array}\right], \tag{4}$$

with state variables ordered as $z^\delta(t) = \left[\bar{x}^\delta(t), \bar{y}^\delta(t), \bar{\theta}^\delta(t), \bar{\omega}^\delta(t), \Delta x^\delta(t), \Delta y^\delta(t), \Delta\theta^\delta(t), \Delta\omega^\delta(t)\right]^{\mathrm{T}}$.

This system is already in a block-triangular form, in which the block on the top of the diagonal, $A_{\text{side-by-side},11}$, has a block-triangular structure, with two zero eigenvalues corresponding to the motion of the center of mass. The average rotation of the pair has a nontrivial dynamics, which is characterized by two real eigenvalues $\frac{\eta}{2}\left(-1 \pm \sqrt{1+\frac{4k_p d}{\eta}}\right)$. One of these eigenvalues is always positive, indicating that perturbations will trigger the exponential growth of the average orientation away from zero. The growth of the average orientation is not accompanied by any change in the relative distance along the X-axis (fifth row of the matrix) that could maintain the side-by-side pattern. As a result, side-by-side swimming is always unstable. The remaining three non-zero eigenvalues of the block on the bottom of the diagonal, $A_{\text{side-by-side},22}$, shape the dynamics of the relative orientation and relative distance along the Y-direction, which, however, bear no effect on the stability of the pattern.

2. Results for A-dipoles

Following the same procedure described in the main text to generate Fig. 2, we obtain calibrated parameters in Fig. 1, from which we do not observe notable differences with respect to the case of the T-dipoles in the main paper. Even less differences are observed when assessing the the predictive power of the model, whereby we recover all the statistical differences determined in Fig. 2 in the main text.

Finally, we report details about stability of in-line swimming for calibrated model parameters on A-dipoles in Fig. 2, mirroring Fig. 4 in the main text. Some qualitative differences can be noted between A- and T-dipoles due to their opposite response to the advective flow. First, using calibrated values of k_p and k_v, we always attain stability for any choice of d above approximately 2/3 BL, rather than 1

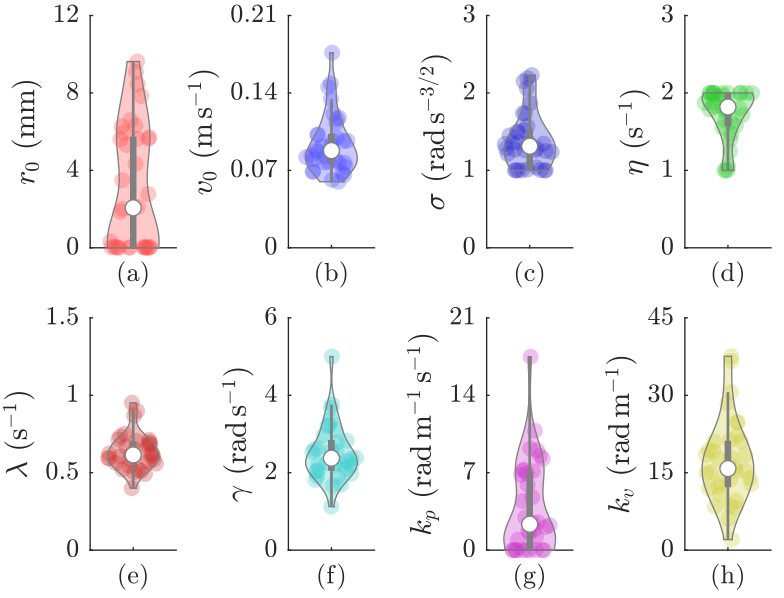

Figure 1. *Calibrated model parameters: (a) characteristic length; (b) speed; (c) baseline activity; (d) mean reversion rate; (e) jump frequency; (f) jump intensity; (g) gain parameter for attraction; and (h) gain parameter for alignment. The colored area in each violin plot is the probability density and coloured circles are individual calibrations. Thick gray bars indicate first and third quartiles; thin gray bars identify minimum and maximum values; and white circles are the median..*

BL as in the main text. Second, for a given value of d, increasing either gain may hamper stability, different frm T-dipoles that seemed to be negatively affected by only large values of k_p.

References

Kanso, E. and Tsang, A. C. H. (2014). Dipole models of self-propelled bodies. *Fluid Dynamics Research*, 46(6):061407.

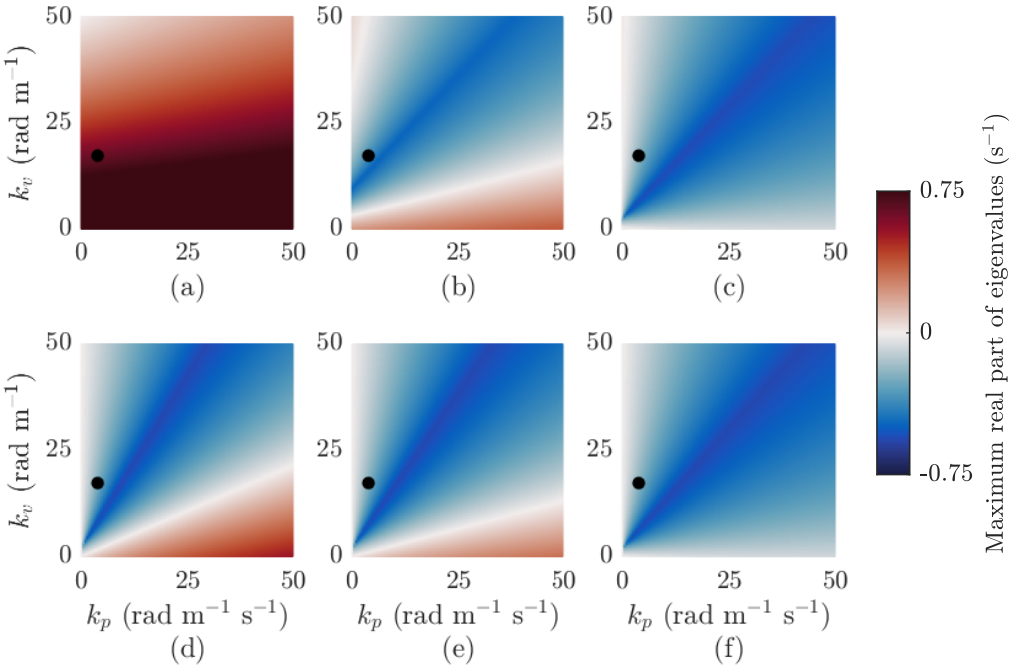

Figure 2. *Stability analysis of in-line swimming as a function of social and hydrodynamic interactions, in the form of heat maps of the maximum real part of the eigenvalues of* $A_{\text{in-line},22}$ *in* (3) *for: (a,b,c)* $r_0 = 3.1$ mm *and (d,e,f)* $r_0 = 0$ mm *(no hydrodynamic interactions). For each of the two scenarios, we consider three values of inter-individual distances d: (a,d) 0.5 BL; (b,e) 1 BL; and (c,f) 2 BL. Other simulation parameters are mean values from Fig. 1:* $\eta = 1.68$ s^{-1}, *and* $v_0 = 0.094$ m s^{-1}. *White regions identify stability boundaries, and black points are mean values from Fig. 1.*